A Feasibility Study of Active Wing/Store Flutter Control

WILLIAM E. TRIPLETT*
McDonnell Aircraft Company, St. Louis, Mo.

Analytical investigations of active feedback flutter control for fighter type aircraft, specifically with respect to wing/store flutter control, show promise of significant benefits for both contemporary and future aircraft. The F-4 Phantom aircraft with an external store is idealized for a flutter critical configuration. Computer programs, based on both frequency and time domains, are used with conventional control system design techniques to generate feedback compensation for active control of flutter for this configuration. Results of linear analyses indicate the possibility of expanding the permissible flight envelope by 150 knots using the existing aileron control surfaces and establish preliminary requirements for control system hardware.

Nomenclature

A, A_c = noncirculatory and circulatory aerodynamic stiffness derivative matrices
B, B_c = noncirculatory and circulatory aerodynamic damping derivative matrices
b = wing reference semichord
C = viscous damping derivative matrix
$C(k)$ = Theodorsen function
g = equivalent structural damping coefficient
I = aerodynamic inertia derivative matrix
i = $(-1)^{1/2}$
K = structural stiffness derivative matrix
$\mathbf{K}$ = control system open loop gain
k = reduced frequency = $\omega b/V$
M = inertia derivative matrix
Q = freestream dynamic pressure
$q_i, \dot{q}_i, \ddot{q}_i$ = generalized coordinates, rates and accelerations with respect to time for both rigid and flexible modes
q_{Fi} = coordinates for degrees of freedom used for excitation
$\{\partial F/\partial q_{Fi}\}$ = column matrices of generalized force in each generalized coordinate mode in response to excitation coordinate q_{Fi}
(θ_{out}/q_{Fi}) = complex frequency response function of displacement, rate or acceleration in response to excitation coordinate q_{Fi}
s = nondimensional time = Vt/b
S = $i\omega$
t, τ = time
V = aircraft forward velocity
α = wing angle of attack attributable to twist—streamwise
δ = aileron deflection angle
$\Phi(s)$ = Wagner function = $1 - A_1e^{-B_1s} - A_2e^{-B_2s}$
ϕ_i = participation coefficients for each generalized coordinate in the response function (θ_{out}/q_{Fi})
ω = excitation frequency
σ = nondimensional time = $V\tau/b$
[ ] = square matrix notation
{ } = column matrix notation

Subscripts

C = command
M = measured
FB = feedback

Introduction

ACTIVE flutter control offers the promise of significant weight benefits in advanced fighter, interceptor, and reconnaissance type aircraft. Design requirements for some of these aircraft include high speed at low altitudes, low load factor, and thin wings. These configurations tend toward flutter critical designs which would require a significant additional weight, even with the optimum use of advanced materials, if passive flutter control were used. Active flutter control offers a potential reduction of this weight penalty. It also offers the promise of a significant expansion of the flight envelope for both contemporary and future aircraft when these vehicles are carrying external stores.

Contemporary fighter aircraft are currently using very sophisticated flight control augmentation systems. The logical development of these systems to fly-by-wire with sensed feedback control can be expected using present sophistication but with enhanced reliability. The development of these systems is being directed primarily toward purposes such as gust alleviation and load attenuation. If these active feedback control systems can be shared by a flutter control system, the weight savings could be very impressive for future aircraft.

The theoretical possibility of feedback control of flutter has been predicted by investigators for many years. One of the first published discussions of the subject appeared in a paper by Pepping[1] in which he postulated the active control of flutter by feedback of a signal for the torsion deflection of an aerodynamic lifting surface. This signal, after compensation, would command the rotation of a control surface to suppress the motion. Other investigators have studied somewhat similar approaches to active flutter control. Theisen and Robinette[2] reported an increase of the flutter speed by 20% for an unswept symmetrical airfoil wind-tunnel model. Forces were applied to the wing by a trailing-edge control surface in response to the torsion mode. The study was only partially successful since control of flutter was lost at the higher velocity; therefore, rapid frequency changes occurred creating a supercritical flutter mode at a higher frequency. Another recent effort is the study by Moon and Dowell.[3] Here the flutter control of a thin cantilevered plate under a transverse follower force is reported. Significant frequency changes were obtained by the use of forces proportional to strain gage signals. Unfortunately, however, there was no significant improvement of flutter since a new instability was generated by phase shifts in the feedback electronics.

This paper reports on an analytical study of the feasibility of active control of wing/store flutter for the F-4 Phantom aircraft. The particular configuration considered in these studies is with the 370 gallon fuel tank on the outboard store station, as shown in Fig. 1. The analytically predicted flutter boundary for this configuration, as a function of the percent fuel load, is shown in Fig. 2. This boundary was investigated by flight flutter testing. A mildly divergent flutter was encountered with the fuel tank near 90% full. Thus, this configuration provides both an analytical and experimental base for the study.

Received November 8, 1971; revision received February 18, 1972. The author wishes to express his appreciation to R. J. Landy for valuable assistance in this study and for the programing of the time domain computer program.

Index categories: Structural Dynamic Analysis; Aircraft Handling, Stability and Control.

* Technical Specialist, Structural Dynamics. Member AIAA.

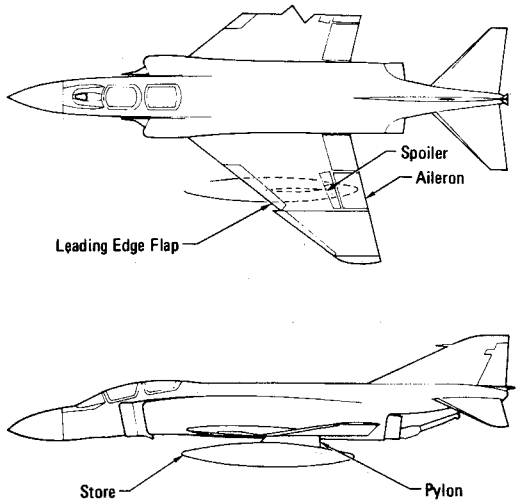

Fig. 1 F-4 with 370 gallon tank.

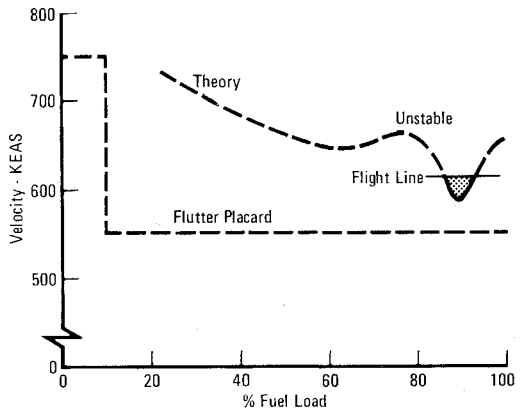

Fig. 2 Flutter boundary—F-4 with 370 gallon tank.

Discussion

An aircraft experiences elastic deformations as a result of turbulence and maneuver loads which occur during flight. A flutter control system must be able to prevent the unstable build up of these deformations even when the aircraft is in a flutter critical region of the flight envelope. This requirement for continuous control of an unstable dynamic system in a turbulent environment is distinctly different compared with the requirements for control of stable dynamic systems. It is one of the principal differences between active flutter control and load alleviation and mode suppression such as the LAMS B-52 study[4] and the XB-70 studies.[5,6] These studies and tests were performed at constant velocity level flight, and the general concept in both cases was to attenuate or damp the structural motion of a stable dynamic system.

Flutter Control Scheme

The control law model of Fig. 3 illustrates the particular active flutter control scheme reported in this paper. For this scheme the reference signal of the control system is a command for the torsion deflection (i.e., angle of attack caused by twist) of the wing to be zero at the location of the sensor. For these studies, an angular accelerometer is used to measure the angular acceleration of all significant vibration modes of the wing. Signals from this sensor are fed back through compensation networks to command the rotation of the aileron. The aileron produces aerodynamic forces which can

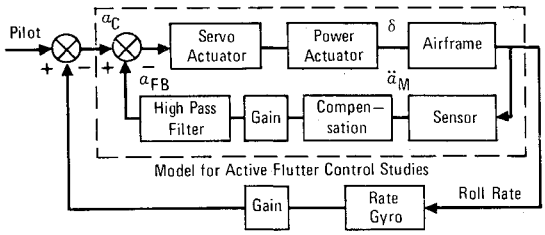

Fig. 3 Control law model.

oppose those forces caused by the angle of attack attributable to twist and thus stabilize the system. If the angle of attack can be continuously nullified, the flutter instability can be precluded. The high pass filter, shown in the figure, has been introduced to filter out static and low frequency angle-of-attack signals associated with the normal aircraft short period mode so that the suppression system affects only the higher frequency flutter modes. The procedure is similar in concept to that suggested by Ref. 1. The control system design procedure here is to create the proper forces in both amplitude and phase to control this vibratory angle of twist motion which varies with airspeed, altitude and other flight parameters.

Analytical Tools

Recently developed computer programs for integrated control-structural dynamics analyses in both the frequency domain and the time domain have been used in these studies. Both programs are designed to evaluate the dynamic stability of a general aeroelastic system considered as an integral part of a multiloop feedback control system.

Frequency domain program

The aeroelastic equations, for both rigid and flexible motion, are expressed in generalized coordinates to fit the symbolic linear equation in the frequency domain.

$$(-\omega^2[M+QI/V^2]+[K+Q[A+A_cC(k)]]+ i\omega[C+(Q/V)[B+B_cC(k)]])\{q\} = \{\partial F/\partial q_{F_1}\}q_{F_1}+\{\partial F/\partial q_{F_2}\}q_{F_2}+\cdots$$

The column matrices on the right are used for the forcing function degrees of freedom. The forcing functions may or may not involve aerodynamics as the user chooses. When the program is used for a linear study, superposition applies and more than one forcing function may be evaluated. For this study, the aileron has been used as the forcing function.

These complex equations of motion are solved simultaneously for a specified airspeed (V) and frequency (ω) to obtain the response of each generalized coordinate to each forcing function. The complex frequency response functions are sensed by arbitrary sensors located at arbitrary points on this arbitrary aeroelastic system by the symbolic equation

$$(\theta_{out}/q_{F_i}) = S^n[\phi_1 q_1/q_{F_i}+\phi_2 q_2/q_{F_i}+\cdots]$$

where n is the response type: $n=0$ gives deflection response; $n=1$ gives rate response; and $n=2$ gives acceleration response. The participation coefficients specify the relative amounts for each generalized coordinate in the sensor response. For this study, the sensor equation generates the angular acceleration at the sensor location as

$$\ddot{\alpha}_M = (-\omega^2)\sum_{i=1}^{N}\phi_i\frac{q_i}{\delta}\delta$$

where N is the number of modes being sensed. These sensor signals then represent the airframe dynamics in a multiloop aircraft control system.

Stability is assessed for the passive aeroelastic system, represented by the left hand side of the equations of motion, by the Mikhailov criterion.[7] An equivalent criterion for the assessment of passive stability is described by Landahl.[8] The stability of the closed loop system is evaluated by the Nyquist criterion.[9] Computer generated plots indicate at a glance both the passive and the closed loop stability.

Time domain program

This program is written in the IBM CSMP[10] (Continuous System Modeling Program) format expressing the aeroelastic equations in symbolic form:

$$M\ddot{q} + C\dot{q} + Kq + QAq + \frac{Q}{V}B\dot{q} + \frac{Q}{V^2}I\ddot{q} +$$

$$QA_c[q(0)\Phi(s) + \int_0^s \frac{dq}{d\sigma}\Phi(s-\sigma)d\sigma] +$$

$$\frac{Q}{V}B_c[\dot{q}(0)\Phi(s) + \int_0^s \frac{d^2q}{d\sigma^2}\Phi(s-\sigma)d\sigma]$$

$$= \left\{\frac{\partial F}{\partial q_{F_1}}\right\}q_{F_1} + \left\{\frac{\partial F}{\partial q_{F_2}}\right\}q_{F_2} + \cdots$$

The time domain program is designed to match the frequency domain program as closely as possible. The convolution integral based on the Wagner function is used to represent the unsteady indicial aerodynamics in the time domain program. The Theodorsen function represents the equivalent unsteady effect in the frequency domain program. Other than this difference there is one-to-one correspondence between the two programs.

The major function of the time domain program is to evaluate the rate, displacement and power demands on the control system in the presence of maneuver and gust loading and to assess the effect of system nonlinearities. It is also useful for final verification of the effectiveness of an active flutter control system designed in the frequency domain.

Aircraft idealization

As mentioned before, the aircraft model for these feasibility studies of active wing/store flutter control is the F-4 with a 370 gallon tank 90% full located on the outboard store station, as shown in Fig. 1. The aileron, which is located at the spanwise station of the store, is used as the force producer. Only existing control surfaces were considered in these studies. In this regard it is interesting to notice that the aileron, spoiler and leading-edge flap are all located at the same spanwise station. Each of these surfaces, either singly or in pairs, is available for use as flutter control force producers.

Vibration data for this configuration are given in Table 1. The model consists of a truncated set of normal modes for the aircraft wing based on measured intertia data and structural influence coefficients. These data are as used in project flutter analyses for external stores. The critical flutter mode for this case is symmetrical so the effect of the rigid motion of the aircraft in translation and pitch is incorporated into the normal mode vibration analysis. The studies were made for half an airplane. The zero airspeed damping shown in the table was measured in ground vibration tests.

Participation coefficients for the angle of twist at the accelerometer location are given in Table 1 for the seven lowest wing modes. The accelerometer is located on the wing in the vicinity of the aileron hinge line. This location was chosen to minimize the interaction or coupling between aeroelastic modes based on the work by Wykes et al.[5]

The Indicial Lift flutter program[11] was used to generate the matrices of aerodynamic derivatives for both the frequency and time domain computer programs and to establish a

Table 1 Aircraft vibration data

Mode description	Frequency Hz	Zero airspeed damping g	Twist coefficient at accelerometer location ϕ_1-rad/ln	Mode normalization point
Pylon roll	5.77	0.020	−0.000736	TE wing tip
Wing 1st bending	7.18	0.025	−0.00264	TE wing tip
Tank pitch-wing torsion	8.78	0.015	0.00200	LE wing tip
Tank yaw	11.40	0.015	0.000308	Rack lateral
Wing 2nd bending	15.61	0.015	−0.0000055	TE wing tip
Outboard wing torsion-wing 3rd bending	35.55	0.015	−0.00113	TE wing tip
Higher mode	37.47	0.015	−0.0178	Aileron hinge

reference passive flutter solution. The seven elastic modes of Table 1 and the aileron rotation mode are included in this case. Flutter occurs for this reference case at a velocity of 525 KEAS (Knots Equivalent Air Speed) and a frequency of 8.3 Hz for $g = 0.0$. It occurs at 550 KEAS for $g = 0.02$ and 585 KEAS for $g = 0.04$. A second instability is indicated at about 1000 KEAS at a frequency of 30 Hz. It was verified by mode deletion studies that the critical passive flutter velocity is determined by the three lowest wing modes only and is not affected by either the aileron rotation mode or the higher frequency wing modes.

Results

Frequency domain studies

A conventional approach to control system design has been used in these studies. The frequency domain computer program, previously described, was used both to verify the passive flutter stability of the open loop system and to evaluate the stability of the closed-loop feedback system for various trial compensation networks. A nine degree-of-freedom representation was used in these frequency domain studies. The degrees of freedom were the seven elastic vibration modes of the wing listed in Table 1, the aileron elastic rotation mode, and the aileron actuator deflection considered as the input forcing function for the aeroelastic equations of motion.

A significant number of trial compensation techniques have been evaluated for the control law model described in Fig. 3. One of the most promising of these techniques is described in this paper. These studies have been made with an improved power actuator with its frequency response extended flat (less than 3 db attenuation) past the flutter frequency being controlled and with the existing power actuator.

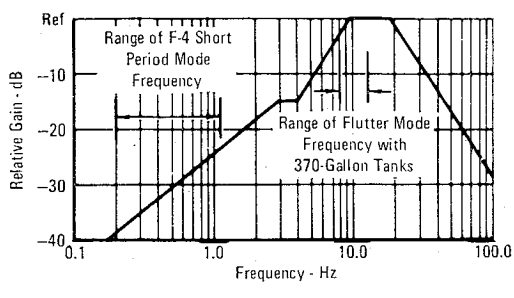

Note: Plot is of High Pass Filter, Power Actuator, and Compensation Only

Fig. 4 Modified Bode diagram for improved power actuator.

Studies with improved power actuator

In equation form, the control system components for this case are

$$\underset{\text{filter}}{\text{High pass}} \quad \underset{\text{actuator}}{\text{Power}} \quad \underset{\text{Comp}}{\text{Lead}}$$

$$K\left(\frac{0.05S}{1+0.05S}\right)\left(\frac{1}{1+0.016S}\right)\left(\frac{117.5+4.61S}{117.5+S}\right)^2 \times$$

$$\underset{\text{Comp}}{\text{Lag}} \quad \underset{\text{grator}}{\text{Inte-}} \quad \underset{\text{acceleration}}{\text{Angular}}$$

$$\left(\frac{59.6+0.0469S}{59.6+S}\right) \times \frac{1}{S^2}\left(S^2 \sum_{i=1}^{7} \phi_i \frac{q_i}{\delta}\right) \times$$

$$\text{Servo actuator}$$

$$\left(\frac{1}{1+[2(0.86)/226]S+S^2/(226)^2}\right) \times$$

$$\text{Accelerometer}$$

$$\left(\frac{1}{1+[2(0.6)/502]S+S^2/(502)^2}\right)$$

A modified Bode[12] plot, in terms of a reference open loop gain of unity, is shown in Fig. 4. This figure is intended to illustrate the method of compensation and is a plot of only the high pass filter, the power actuator and the compensation networks. The actual design of the control system is done with Nyquist plots, since for the coupled aeroelastic system the angular acceleration of the aeroelastic modes is known only in terms of an amplitude and phase at each frequency and has no convenient analytical formulation. The servo actuator and the angular accelerometer are both well separated from the primary frequency range of interest which is in the neighborhood of 8–9 Hz.

The general approach is to add enough phase lead to the closed-loop system to control the unstable flutter mode. This phase lead is followed by phase lag to prevent the destabilization of the passively stable higher frequency modes. As seen in Fig. 4, the high pass filter, which is unity above 3 Hz, effectively decouples the flutter control system from the flight control system. The improved power actuator, which breaks down at 10 Hz, and the high pass filter control the response up to 4 Hz, which is the lower break frequency for the phase lead compensation. The gain increases at 40 db/decade until the phase lag compensation takes effect at 9.5 Hz to create the plateau. The attenuation for higher frequencies begins at the phase lead upper break frequency of 19 Hz.

Modified Nyquist plots of the characteristic equation of the closed-loop feedback system (based on the origin rather than the minus one point) are shown in Fig. 5 for an open loop gain of 2.0 and a structural damping coefficient of $g = 0.04$. Plots are shown for six aircraft velocities from 200 KEAS–800 KEAS. Passive flutter occurs between 550 and 600 KEAS as indicated by the change in the direction of closure for the trajectory from clockwise below flutter onset to counter-clockwise above flutter onset. After flutter onset, two poles are present in the right half plane (one for both positive and negative frequencies). The Nyquist criterion requires two counter-clockwise encirclements of the origin to ensure that there are no zeros in the right half plane and thus indicate a stabilized system. The six plots of Fig. 5 indicate a stable system for all velocities through 800 KEAS.

An enlarged Nyquist plot for the velocity of 700 KEAS is shown in Fig. 6. This figure illustrates the type of data from which a control system may be designed. The diagram shows trajectories for three values of the structural damping

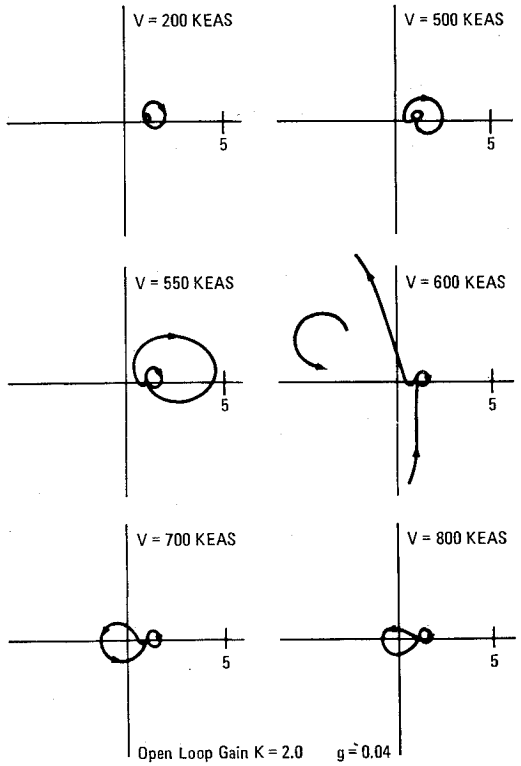

Fig. 5 Modified Nyquist plots for improved power actuator.

coefficient. The phase margin varies from 18° for $g = 0.0$ to 57° for $g = 0.04$. The phase lead compensation was chosen to place the flutter frequency of 8.3 Hz very near the negative real axis to give the greatest latitude on gain adjustment. The maximum possible open loop gain is determined by the crossover at 6.8 Hz. If the gain is increased so that the crossover occurs on the negative real axis, the net number of encirclements of the origin would be zero and thus the system would be unstable. The minimum necessary open loop gain, on the other hand, is determined by the crossover near 8.3 Hz. If the gain is reduced so that this crossover is on the positive real axis, the system would again be unstable.

The stability boundaries for this case with an improved power actuator are shown in Fig. 7. The reference gain for the Nyquist plots is near the bottom of the design window. It is seen that a reduction of open loop gain by a factor of 0.6 is possible, without losing control, at the velocity of 700 KEAS, based on the zero airspeed structural damping coefficient of 0.015.

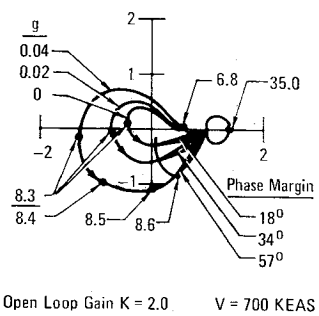

Fig. 6 Modified Nyquist plot for improved power actuator.

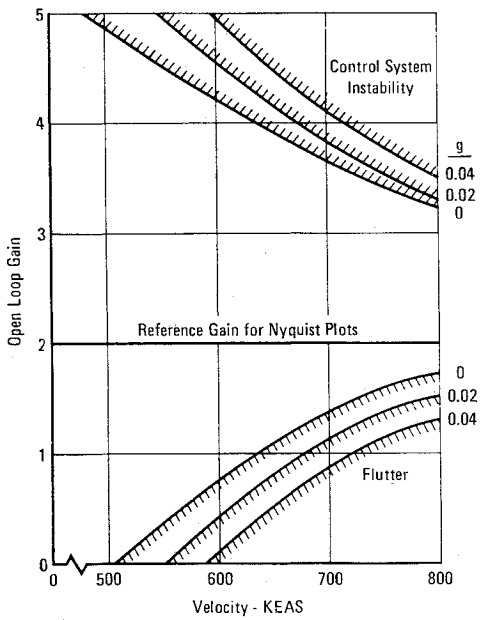

Fig. 7 Stability boundaries with improved power actuator.

Studies with existing power actuator

In equation form, the control system components for this case are

$$\underset{\text{High pass filter}}{\left(\frac{0.05S}{1+0.05S}\right)}\underset{\text{Power actuator}}{\left(\frac{1}{1+0.1S}\right)}\underset{\text{Lead Comp}}{\left(\frac{117.5+4.61S}{117.5+S}\right)^2}\times$$

$$\underset{\text{Lag Comp}}{\left(\frac{59.6+0.0469S}{59.6+S}\right)}\times\underset{\text{Inte-grator}}{\frac{1}{S^2}}\underset{\text{Angular acceleration}}{\left(S^2\sum_{i=1}^{7}\phi_i\frac{q_i}{\delta}\right)}\times$$

$$\underset{\text{Servo actuator}}{\left(\frac{1}{1+[2(0.86)/226]S+S^2/(226)^2}\right)}\times$$

$$\underset{\text{Accelerometer}}{\left(\frac{1}{1+[2(0.6)/502]S+S^2/(502)^2}\right)}$$

A modified Bode plot is shown in Fig. 8 for this control law with the existing power actuator which breaks down at 1.6 Hz. The only change between the control systems of Figs. 4 and 8 is in the power actuator. This change gives about 15 db decrease of relative open loop gain at the flutter frequency of 8.3 Hz. An increase in the open loop electrical gain by 15 db (a factor of 5.625) to $K = 11.25$ will compensate for this loss of mechanical gain and give the same open loop gain as for the improved power actuator case.

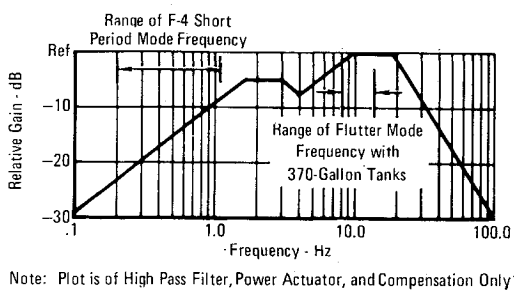

Fig. 8 Modified Bode diagram for existing power actuator.

The Nyquist plots of Fig. 9 indicate a stable system for an open loop gain of 25.0 and a structural damping coefficient of $g = 0.04$ for all velocities through 800 KEAS. Figure 10 shows an enlarged Nyquist plot for the velocity of 700 KEAS. The phase margin for this design is 27° for $g = 0.04$, but only 9° for $g = 0.02$. The system is unstable for $g = 0.0$. The stability boundaries, shown in Fig. 11, indicate that the open loop gain could be reduced to 11.25 for a structural damping coefficient of $g = 0.02$ at a velocity of 700 KEAS without losing control of flutter.

More phase lead could be added to this nonoptimum control loop to bring the flutter frequency near the negative real axis on the Nyquist plots. This would give the maximum latitude on gain adjustment as well as increased phase margins as illustrated by Figs. 4–7 for the improved power actuator case.

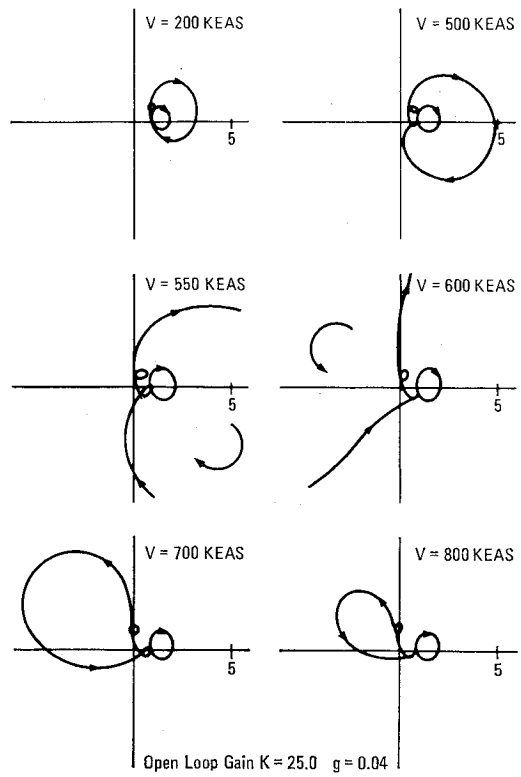

Fig. 9 Modified Nyquist plots for existing power actuator.

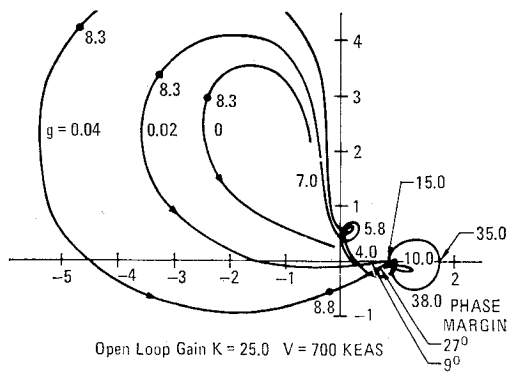

Fig. 10 Modified Nyquist plot for existing power actuator.

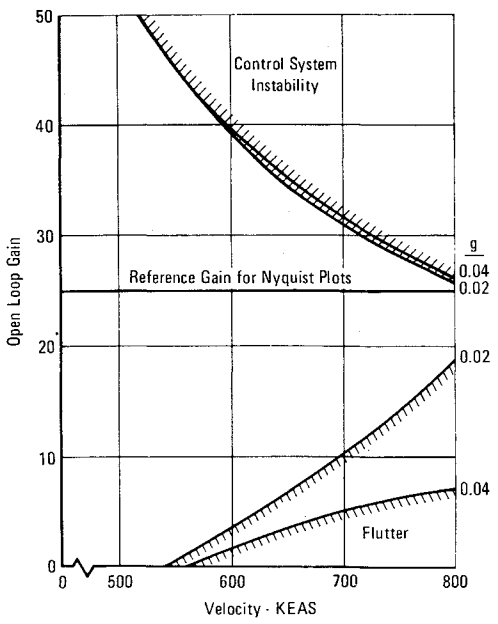

Fig. 11 Stability boundaries with existing power actuator.

Time Domain Studies

The time domain computer program, previously described, has been used to verify the effectiveness of the active flutter control system designed in the frequency domain. Linear studies with this program also give the deflection and rate requirements for the aileron actuator for various types and amplitudes of initial excitation. For these time domain studies the number of degrees of freedom are restricted to the three lowest elastic vibration modes of the wing, listed in Table 1. The actuator deflection is the forcing function for the aeroelastic equations of motion. The Wagner function coefficients are $A_1 = 0.165$, $A_2 = 0.335$, $B_1 = 0.0455$, and $B_2 = 0.3$. The control system is the time domain equivalent of the improved power actuator case.

Stability verification

The starting excitation used for stability verification is in the form of an impulse acting for a very short period of time. This form of excitation has been chosen because of the broad frequency content of this shape. Each of the vibration modes is given significant deflections as a result of this excitation so that flutter stability may be assessed by short runs on the computer.

Sample time history printouts from the time domain program are shown in Fig. 12 for an impulse of 80,000 lb for 0.01 sec at a velocity of 700 KEAS. This input creates maximum deflections of 5.4 in. at the wing tip in the flutter mode. To control the inherently unstable motion requires a maximum aileron deflection of 5.7° with the improved power actuator design. The effective damping coefficient in the flutter mode is $g = 0.027$. For an open loop gain increased to $K = 2.5$ the aileron deflection is 6.9° with an effective damping of $g = 0.067$ in the flutter mode. These runs verify the system stability for actuators with unlimited capability when deep in the flutter region.

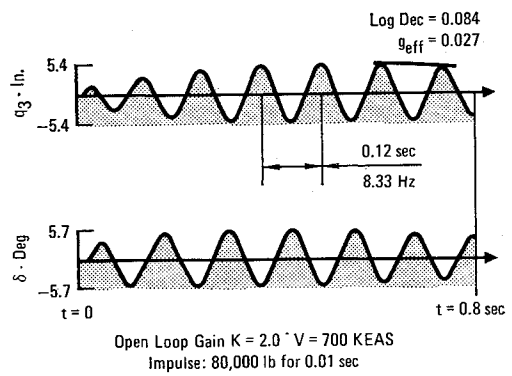

Fig. 12 CSMP printout—improved power actuator-impulse excitation.

Preliminary aileron deflection and rate requirements

The starting excitation used to determine the preliminary aileron design requirements is a discrete gust of the form (1–cos). This form was chosen to allow an evaluation of the response for excitation matching the aircraft short period mode and flutter frequencies.

A gust wave length of 1180 ft is chosen to give a gust period of 1 sec at a speed of 700 KEAS for the traces of Fig. 13a. The gust force amplitude of 70,000 lb represents a 30 fps discrete gust for a minimum weight F-4 aircraft. This low frequency gust allows the flutter control system to "ride out" the disturbance and maintain stability with aileron deflections of less than 1° and rates of less than 10 deg/sec. This run verifies that maneuver loads and high intensity gusts in the frequency range of 1–2 Hz create minimal demands on the flutter control system.

A discrete gust at the flutter frequency creates a much more demanding environment as shown in Fig. 13b. The input gust force here has a period of 0.12 sec, a wave length of 142 ft (8.8 times the mean aerodynamic chord) and an amplitude of 10,000 lb. The amplitude was obtained by integration over the bandwidth of the flutter mode (8.0 to 8.7 Hz) under power spectral density curves representing flight through a typical thunderstorm (root mean square velocity = 13.38 fps).

The maximum aileron deflection of 2.2°, shown in Fig. 13b, is well within the capabilities of the F-4 aileron. Hinge moment limitations allow up to 10° of aileron deflection over the entire flight domain. The maximum aileron rate of 113 deg/sec, however, is approximately equal to the existing no-load rate capability. Some reserve must be provided to accommodate steady aileron loads.

The required aileron rates may be reduced by decreasing the open loop gain of the control system without losing control of the flutter mode. This, however, will reduce the damping in the controlled mode and thus require significant aileron deflections for longer periods of time after a disturbance.

A preliminary evaluation of the possibility of increasing the aileron rate limit indicates the practical maximum to be

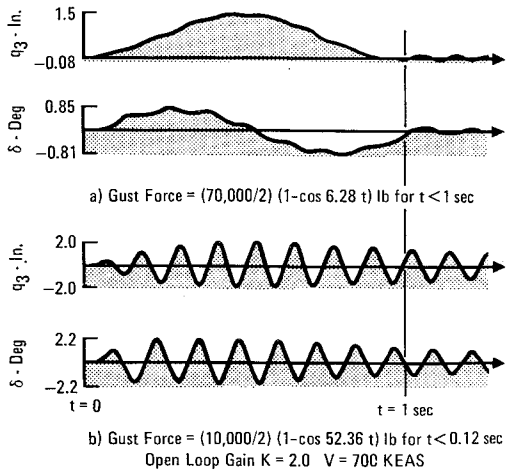

Fig. 13 CSMP printout—improved power actuator-(1–cos) excitation.

on the order of 200 to 300 deg/sec. The concept of using an accumulator with the present system capacity offers a distinct design possibility for effectively increasing the rate capability to more than 400 deg/sec for short-term demands.

These feasibility studies give some indication of realistic rates for the aileron actuator based on linear analyses. The final design requirements should be based on more refined analysis including the system nonlinearities.

Conclusions

A general approach to the design of an active flutter control system for fighter aircraft wing/store flutter control has been illustrated. The design is accomplished using conventional control system design techniques in the frequency domain. Active control is based on the use of the aileron to create aerodynamic forces with the proper amplitude and phase to oppose those forces caused by the wing angle of attack attributable to twist, and thus stabilize the motion. The system can "ride out" maneuver loads and gusts in the frequency range of 1–2 Hz or less, but excitation in the neighborhood of the flutter frequency creates significant rate demands on the hydraulic actuators.

This investigation has established, on the basis of linear analyses, the feasibility of active control of F-4 wing/store flutter for a 370 gallon tank 90% full, using an improved aileron power actuator. The studies with the existing aileron power actuator are promising, but are less complete, so the feasibility is not as conclusive. The time domain studies have established preliminary sizing requirements for the improved power actuator case.

These studies are the first steps in the design of an active flutter control system for wing/store flutter. Additional studies of feasibility and to establish design requirements include: 1) further evaluation of the feasibility of using the existing power actuator; 2) the evaluation of the complete effects of nonlinearities on both the stability and response of the aircraft; 3) the assessment of the required power to avoid control system saturation during flight through severe turbulence or during excessive maneuvers; 4) the assessment of changes in aircraft performance resulting from system modifications for flutter control; 5) the evaluation of the ability of a single compensation design to control flutter for several store configurations, including other fuel loads for the 370 gallon tank; and 6) the evaluation of other promising flutter control concepts.

References

[1] Pepping, R. A., "A Theoretical Investigation of the Oscillating Control Surface Frequency Response Technique of Flight Flutter Testing," *Journal of the Aeronautical Sciences*, Vol. 21, No. 8, Aug. 1954, pp. 533–542.

[2] Theisen, J. G. and Robinette, W. C., "Servo-Control of Flutter," ASME/AIAA 10th Structures, Structural Dynamics, and Materials Conference, New Orleans, La., April 1969.

[3] Moon, F. C. and Dowell, E. H., "The Control of Flutter Instability in a Continuous Elastic System Using Feedback," ASME/AIAA 11th Structures, Structural Dynamics, and Materials Conference, Denver, Colo., April 1970.

[4] "Aircraft Load Alleviation and Mode Stabilization (LAMS)," AFFDL-TR-68-158, Dec. 1968, The Boeing Co., Seattle, Wash., and Honeywell Inc., Minneapolis, Minn.

[5] Wykes, J. H. and Mori, A. S., "An Analysis of Flexible Aircraft Structural Mode Control," AFFDL-TR-65-190, Pt. I, June 1966, Air Force Flight Dynamics Lab., Wright-Patterson Air Force Base, Ohio.

[6] Wykes, J. H., Nardi, L. U., and Mori, A. S., "XB-70 Structural Mode Control System Design and Performance Analyses," CR-1557 July 1970, NASA.

[7] Mikhailov, A. V., "Harmonic Analysis in the Theory of Automatic Control," *Automatika i Telemkhanika*, Moscow, 1938.

[8] Landahl, M. T., "Graphical Technique for Analyzing Marginally Stable Dynamic Systems," *Journal of Aircraft*, Vol. 1, No. 5, 1964, pp. 293–299.

[9] Nyquist, H., "Regeneration Theory," *Bell System Journal*, Vol. II, Jan. 1932, pp. 126–147.

[10] "System/360 Continuous System Modeling Program—Users Manual (H20-0367)," IBM Corp., White Plains, N.Y.

[11] Ferman, M. A., Burkhart, T. H., and Turner, R. L., "First Quarterly Report for Conceptual Flutter Analysis, BuWeps Contract W66-0298-c," Rept. E549, McDonnell Aircraft Co., St. Louis, Mo., 1966; also Code AIR-604AI, Naval Air Systems Command, Dept. of Defense, Washington, D.C.

[12] Bode, H. W., *Network Analysis and Feedback Amplifier Design*, Van Nostrand, New York, 1945.